Critical Analysis of the Phase Behavior of Poly(ϵ-caprolactone) (PCL)/Polycarbonate (PC) Blends

Y. Wilson Cheung*,† and Richard S. Stein*

Department of Polymer Science and Engineering, University of Massachusetts, Amherst, Massachusetts 01003

Received December 20, 1993®

ABSTRACT: The phase behavior and miscibility of poly(ϵ-caprolactone) (PCL)/polycarbonate (PC) blends have been investigated with DSC, cloud-point measurement, TGA, FTIR, NMR, and small-angle neutron scattering (SANS). Thermal analysis results indicated that the PCL-rich blends are semicrystalline/semicrystalline at room temperature. At about 30% PC incorporation, the PCL crystallinity showed a marked reduction, whereas the PC crystallinity approached a maximum. The composition dependence of T_g exhibited a discontinuity (cusp) and was critically analyzed using the classical equations of Gordon–Taylor and Fox and the free volume theory of Braun–Kovacs. Combination of the Fox and Braun–Kovacs equations accurately reproduced the T_g–composition dependence. Thermal stability of the blends, as measured by the onset degradation temperature in air, increased with increasing PC. FTIR results coupled with ^{13}C NMR findings supported the hypothesis that the blends primarily degraded via thermally-induced chain scission of PCL as evidenced by the evolution of CO_2. SANS studies on the deuterated PC-rich blends revealed that the scattering intensity first remained fairly constant with increasing temperature and then increased sharply at temperatures above the blend T_g. The sudden rise in the scattering intensity was attributed to crystallization of PC resulting from prolonged annealing. Results derived from the RPA analysis of the SANS profiles measured at 30 °C for the deuterated PC-rich blends and those obtained from the melting point depression analysis of the PCL-rich blends suggested favorable blend interactions as reflected by the negative sign of the χ parameter.

Introduction

Poly(ϵ-caprolactone) (PCL) is known to be miscible with numerous polymers[1] including poly(vinyl chloride) (PVC), poly(hydroxy ether), chlorinated polyether, and Bisphenol A polycarbonate (PC). PCL is also biodegradable and exhibits a relatively low glass transition temperature T_g (~−60 °C) and melting temperature T_m (~60 °C). Bisphenol A polycarbonate (PC) is one of the toughest polymers and exhibits a fairly high T_g (~150 °C) and T_m (~230 °C). It is expected that blending of these two homopolymers could result in interesting phase behavior which could lead to a modification of their physical properties.

The phase behavior of the PCL/PC blends has been probed with differential scanning calorimetry (DSC), dynamic mechanical analysis (DMA),[2] and Fourier transform infrared spectroscopy (FTIR)[3] and examined with melting point depression analysis.[4] On the basis of these studies, the PCL/PC blend system was found to be miscible over the entire composition range as evidenced by the presence of a single glass transition temperature T_g. This system exhibited a lower critical solution temperature (LCST) at about 260 °C at which demixing was observed. Additionally, PC was found to crystallize in blends containing more than 50% PCL. These PCL-rich blends undergo multiple phase transitions and exhibit very rich and complex morphologies. Unique to the PCL-rich blends is the three-phase morphology in which two distinct crystalline phases (PCL and PC) coexist with a mixed amorphous phase. Athermal and isothermal crystallization kinetics of PCL in the PCL-rich blends have been investigated with synchrotron small-angle X-ray scattering (SAXS),[5] DSC, and optical microscopy.[6] The crystalline morphologies in both the semicrystalline/semicrystalline and semicrystalline/amorphous states have been examined with small-angle neutron scattering (SANS)[7] and quantitative SAXS.[8]

Calorimetric study of low molecular weight analogs of PC and PCL[9] revealed a negative heat of mixing, indicating the presence of specific interactions. This exothermic interaction was attributed to the n–π complex formation between the electrons of the ester carbonyl and the aromatic ring of the carbonate molecule. Results[10] derived from the FTIR studies corroborated the presence of specific interactions of these two components in the amorphous state. The nature of the specific interactions was analogous to that of the PCL/PVC system[11] in which the frequency shifts for both the crystalline and amorphous ν_s(C=O) were observed.

Polymer blend miscibility is commonly measured in terms of the Flory–Huggins interaction (χ) parameter. Numerous techniques including melting point depression,[12] inverse gas chromatography,[13] small-angle neutron scattering,[14,15] and Hess's law calorimetry have been applied to measure χ. Melting point depression, due to its simplicity, is one of the most widely used techniques for χ determination. This approach is based on the assumption that the melting point depression is caused by the thermodynamics of mixing of the miscible polymers. However, morphological effects such as changes in the lamellar thickness due to blending, the degree of crystalline perfection, and the physical nature of the amorphous phase surrounding the crystalline phase can affect the melting point and thus render the analysis questionable. Three different studies have been reported in the literature regarding the value of χ. The first cited an interaction parameter of −1 to −2.[3] From the exothermic heats of mixing between small molecules similar to PC and PCL, the second study[9] reported χ to be between −0.2 and −0.3. The most recent study[4] estimated the interaction parameter to be $0 \sim \chi \leq \chi_{crit}$ (0.024) based on the finding that the PCL-rich blends showed melting endotherms and

† Present address: Dow Chemical Co., Midland, MI 48674.
® Abstract published in *Advance ACS Abstracts*, April 1, 1994.

0024-9297/94/2227-2512$04.50/0

Table 1. Molecular Weights for Poly(ε-caprolactone) (PCL), Hydrogenous Polycarbonate (h-PC), and Deuterated Polycarbonate (d-PC)

polymer	M_w	M_n	M_w/M_n
PCL	23 700	16 500	1.44
h-PC	23 100	36 400	1.57
d-PC	109 000	52 800	2.06

Hoffman–Weeks extrapolations identical to those of the PCL homopolymer.

In order to clarify these ambiguities and to establish a better understanding of this complex blend system, the phase behavior and the miscibility will be critically examined. DSC and cloud-point measurements were employed to identify the various phase transitions. The composition dependence of the glass transition temperature will be analyzed in terms of the classical equations based on the free volume hypothesis and the free volume theory of Kovacs. Thermal stability of the blends at temperatures close to the LCST was assessed with FTIR and thermogravimetric analysis (TGA). Due to the thermal instability of PCL at elevated temperatures close to the LCST, the blends may undergo chain scission and/or transesterification. Nuclear magnetic resonance (NMR) spectroscopy was used to evaluate the chemical integrity of the blends. Attempts will be made to reexamine the equilibrium melting point of the PCL-rich blends. Miscibility between PCL and deuterated PC in the PC-rich blends was probed with small-angle neutron scattering.

Experimental Section

Both PCL and PC were obtained from Scientific Polymer Products. The deuterated PC (d-PC) was synthesized by solution polymerization of deuterated bisphenol with phosgene at 0 °C in methylene chloride.[7] The molecular weights of the these homopolymers, determined from gel permeation chromatography, are shown in Table 1. The two homopolymers were dissolved and mixed in methylene chloride, yielding a 5 wt % solution. The blends were subsequently recovered from solution by precipitating them in methanol. The blends were first air dried overnight and then vacuum dried at 90 °C for 2 days. Pure PCL was subjected to similar purification procedures and thermal treatments. In order to promote solution-induced crystallization, PC was first dissolved in methylene chloride, yielding a 5 wt % solution. The sample was then solution cast on a Teflon-coated surface. The cast films were dried in a manner similar to that of the blends.

Thermal transitions of the blends were measured with a DuPont-10 differential scanning calorimeter at a heating rate of 20 °C/min. The glass transition temperatures were obtained from the second heating scan and determined from the midpoint of the change in heat capacity. The melting endotherms of both components were recorded from the first heating scan, and the melting point was obtained from the peak temperature of the endotherm. On the basis of the values of the heat of fusion for 100% crystalline PC[16] (35.3 cal/g) and PCL[17] (32.4 cal/g), the degree of crystallinity of both PC and PCL was calculated from the melting endotherm and normalized with respect to the composition of each component in the blend.

Due to the large difference in the refractive index between PCL (n = 1.149) and PC (n = 1.586), the optical cloud-point method based on turbidity measurement was used to determine the phase separation temperature. The cloud-point apparatus consisted of a He–Ne laser, hot-stage, photomultiplier tube interfaced to a computer. The scattered light produced from total internal reflection was collected with a photomultiplier detector as shown in Figure 1. This geometry is superior to the conventional turbidity technique as a much wider angular range of scattered light is sampled by this apparatus. The sample was heated to above the blend T_g and cast between two glass slides. The sample was first equilibrated at 240 °C for 3 min on a hot stage and then ramped at 4 °C/min to above the cloud point while the intensity of the scattered light was monitored simultaneously. The temperature at which the scattered light intensity increased significantly was recorded as the phase separation temperature (cloud point). In order to examine the reversibility of the phase separation, the sample was cooled at 4 °C/min to below the cloud point.

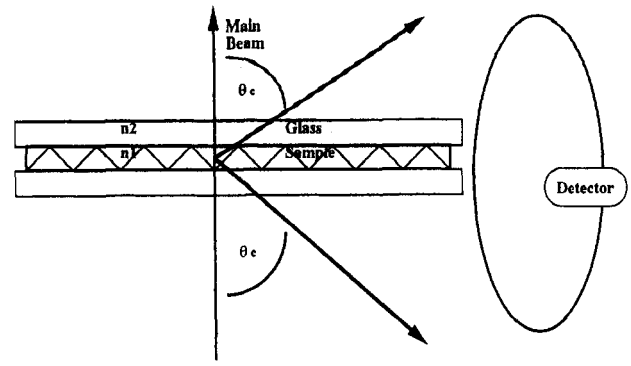

Critical Angle for Total Internal Relection

$n_1 \sim 1.5$, $n_2 \sim 1.2$

$\theta_c = \sin^{-1}(n_2/n_1) = 53°$

Total Internal reflection Occurs at

$\theta_c < \theta < 180 - \theta_c$ or $53° < \theta < 127°$

$q = (4n\pi/\lambda_0) \sin(\theta/2)$

$= 13.3 - 26.7\ \mu m^{-1}$

Figure 1. Cloud-point apparatus analysis: schematics of the wide-angle scattering generated from the total internal reflection.

Thermal stability to the blends was assessed with a Perkin-Elmer TGS2 thermogravimetric analyzer (TGA). The sample was first ramped to 100 °C and then heated at 10 °C/min to 600 °C. Measurements were conducted in air. FTIR was performed on samples cast on NaCl plates with an IBM-32 spectrometer averaging 128 scans. ^{13}C NMR was performed on samples dissolved in chloroform with a Varian 300 XL spectrometer.

SANS samples were prepared by dissolving the two components, PCL and d-PC, in methylene chloride. The blend solution was then cast on an aluminum surface. The samples were first dried under ambient conditions overnight and then were vacuum dried at 90 °C for 2 days to ensure complete removal of residual solvent. In order to destroy the thermal history and to render the blends amorphous, the samples were heated to 250 °C for 3 min under vacuum. Scattering samples were typically compression molded at T_g + 50 °C under vacuum. Samples were then rapidly transferred to a metal surface and quenched to room temperature. Sample disk dimensions were about 1 mm in thickness and 15 mm in diameter.

SANS experiments were performed at the National Institute of Standards and Technology (NIST), Gaithersburg, MD. Measurements were conducted on the 30-m CHRNS SANS instrument. The neutron wavelength was 5 Å ($\Delta\lambda/\lambda$ = 0.34), and the source and sample slits were separated by a distance of 14.77 m. The sample–detector distance was 12.5 m, and the data were corrected for instrumental backgrounds and detector efficiency on a cell-by-cell basis, prior to radial averaging to give a q-range of 0.0013–0.044 Å^{-1}. The net intensities were converted to an absolute (±5%) differential cross section per unit sample volume (in units of cm^{-1}) by comparison with precalibrated secondary standards.[18] Incoherent scattering backgrounds were estimated from the scattering of the hydrogenous polymers and were subtracted from the sample scattering.

Results and Discussion

Phase Transitions. The "quasi-equilibrium" (due to kinetic effects) phase diagram for the PCL/PC blends is depicted in Figure 2. As discussed earlier, the phase transitions were measured at 20 °C/min with the exception of the lower critical solution temperature (LCST) which was measured at 4 °C/min. In accord with previous results,[2-4] this blend system is miscible in the amorphous phase, as demonstrated by the presence of a single glass transition temperature, over the entire composition range. Both PCL and PC in the PCL-rich blends readily undergo crystallization under ambient conditions. Therefore, PCL

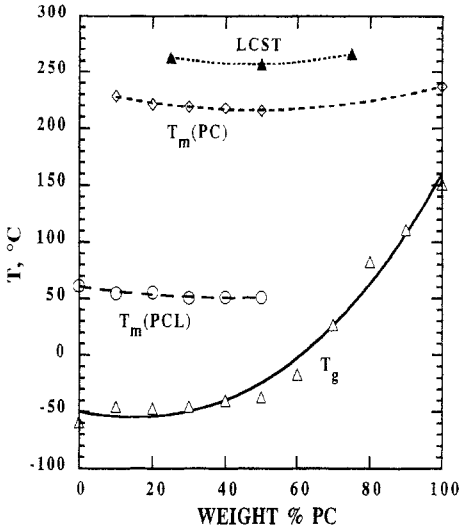

Figure 2. Phase transition temperatures for PCL/PC blends measured at 20 °C/min. The lower critical solution temperature (LCST) was obtained at 4 °C/min.

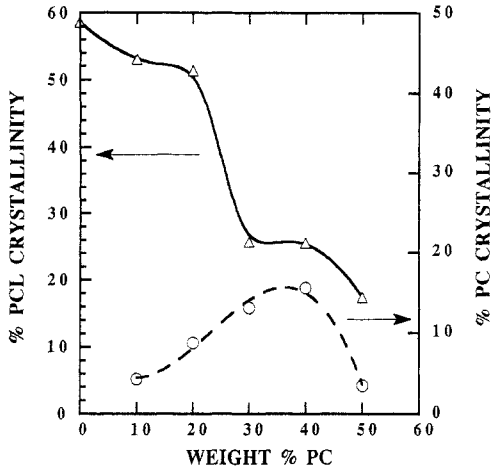

Figure 3. Normalized PCL and PC crystallinity, obtained from quenching the samples from above the melting point of PC to room temperature, for the PCL-rich blends.

is an effective macromolecular plasticizer for PC as pure PC cannot crystallize at temperatures below 150 °C. Figure 3 shows the normalized PCL and PC crystallinites, obtained from quenching the blends from above T_m of the respective component to room temperature, for the PCL-rich blends. At about 30% PC incorporation, it was observed that the PCL crystallinity, for blends crystallized either athermally or isothermally,[6] showed a marked reduction, whereas the PC crystallinity approached a maximum. Crystallization of both components was strongly suppressed in the PC-rich blends.

Cloud-point measurements indicated that the blends experienced phase separation above the LCST. As the sample approached its phase separation temperature, the integrated scattering intensity increased sharply as depicted in Figure 4. This temperature is termed the cloud point and is related to the binodal curve. In the limit of infinitely slow heating rate and monodisperse molecular weight distribution, the cloud-point curve corresponds to the locus of the binodal curve.[19] As indicated in this figure, the integrated scattering intensity decreased as the sample was cooled below the cloud point and such reversibility was a strong signature of a true LCST.

Glass Transition Temperature Analysis. Blend miscibility is often quantified by measuring the blend T_g and by analyzing its dependence with composition. Traditionally equations[20-23] based on the free volume hypothesis have been used to model the composition dependence of the glass transition temperature. The two mostly used expressions are the Fox[20] and the Gordon–Taylor[23] equations. The Fox equation shown below

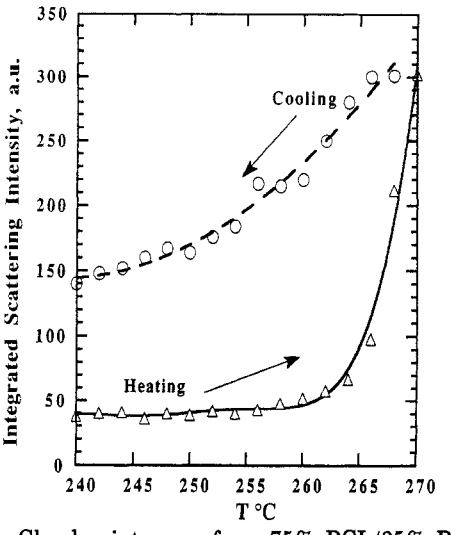

Figure 4. Cloud-point curve for a 75% PCL/25% PC blend ramped at 4 °C/min.

$$\frac{1}{T_g} = \frac{W_1}{T_{g1}} + \frac{W_2}{T_{g2}} \tag{1}$$

where W_i is the weight fraction of component i and T_g is the blend T_g, assumes the specific heats of the two components are identical. The Gordon–Taylor equation

$$T_g = \frac{W_1 T_{g1} + k W_2 T_{g2}}{W_1 + k W_2} \tag{2}$$

where $k = \Delta\alpha_{p2}/\Delta\alpha_{p1}$, and $\Delta\alpha_{pi}$ is the difference in the thermal expansion coefficient between the liquid and glassy states at T_{gi}, accounts for the effects of thermal expansion on the T_g. In general, k is often used as a fitting parameter. These classical equations predict that T_g increases continuously (smoothly) and monotonically with composition.

However, it has been observed that the T_g–composition variation of several polymer blend systems is not monotonic and exhibits a cusp at certain critical composition.[24] This phenomenon becomes very prominent when the T_g difference between the two homopolymers exceeds 50 °C. The classical equations become invalid below a critical temperature T_c as the free volume of the high T_g component becomes zero. According to Kovacs,[25] the critical temperature and composition are given by

$$T_c = T_{g2} - (f_{g2}/\Delta\alpha_2) \quad \text{if} \quad T_{g2} > T_{g1} \tag{3}$$

$$\phi_c = \frac{f_{g2}}{[\Delta\alpha_1(T_{g2}-T_{g1}) + f_{g2}(1 - \Delta\alpha_1/\Delta\alpha_2)]} \tag{4}$$

where $\Delta\alpha_2$ is the difference between the volume expansion coefficients in the glassy and liquid states of component 2 and f_{g2} is the free volume fraction of polymer 2 at T_{g2}. Below T_c, the T_g is described by

$$T_g = T_{g1} + \left(\frac{f_{g1}}{\Delta\alpha_1}\right)\left(\frac{\phi_2}{\phi_1}\right) \tag{5}$$

According to this equation, the blend T_g is uniquely determined by the properties of the low T_g polymer at temperatures below T_c or at compositions below ϕ_c. If

Table 2. Composition, Degree of Crystallinity, and Glass Transition Temperature of PCL/PC Blends

wt % PC	% PC crystallinity	% PCL crystallinity	ϕ_{PC}[a]	T_g, K
0.0	0.0	58.6	0.0	213.8
0.1	4.3	53.0	17.1	227.5
0.2	8.8	51.3	29.9	226.0
0.3	13.1	25.6	31.3	227.7
0.4	15.6	25.5	40.8	233.0
0.5	3.5	17.3	51.5	235.9
0.6	0	1.9	57.9	256.0
0.7	0	0	68.0	299.8
0.8	0	0	78.5	355.6
0.9	0	0	89.1	384.2
1.0	0	0	100.0	424.0

[a] Volume fraction of PC in the mixed amorphous phase.

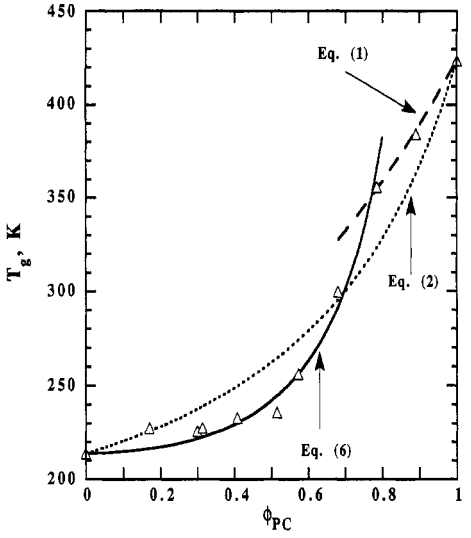

Figure 5. Glass transition temperature for PCL/PC blends as a function of volume fraction of amorphous PC in the mixed amorphous phase. T_g–composition dependence analysis: Eq. (1), Fox; Eq. (2), Gordon–Taylor with k = 0.27; Eq. (6), Braun–Kovacs with g = 0.0227.

there is excess volume between the two polymers upon mixing, Braun and Kovacs[26] have derived the following:

$$T_g = T_{g1} + \frac{\phi_2 f_{g2} + g\phi_1\phi_2}{\phi_1 \Delta\alpha_1} \tag{6}$$

where g is an interaction term defined as

$$g = \frac{(V_e/V)}{\phi_1\phi_2} \tag{7}$$

where V_e is the excess volume and V the volume of the blend. The excess volume or g is positive if blend interactions are stronger than those between the homopolymers. Effectively, g is obtained by fitting the T_g–composition data to the Braun–Kovacs equation.

The overall weight fraction, normalized PCL and PC crystallinities, volume fraction, and the corresponding T_g are listed in Table 2. From the degree of crystallinities and the density value of 1.095 g/cm^3 for amorphous PCL[17] and 1.196 g/cm^3 for PC,[16] the real composition, expressed in terms of the volume fraction of PC, of the amorphous phase was calculated and plotted in Figure 5. Three different equations were applied to model the T_g–composition dependence. The Gordon–Taylor fit to the data yielded a k value of 0.27 and failed to reproduce the cusp observed in the T_g–composition variation. On the basis of the classical value of 0.025 for f_{g2} and 0.00048 K^{-1} for $\Delta\alpha_2$, the critical temperature and volume fraction (with respect to PC) are 372 K and 0.72, respectively. The Fox equation was used to fit the data above ϕ_c, and the Braun–Kovacs equation was applied to the data below ϕ_c. Combination of the Fox equation and the Kovacs theory accurately predicted the T_g–composition variation. It was found that the Braun–Kovacs fit yielded a g value of −0.0227. This negative value suggested that the blend interactions are fairly weak. Additionally, the crossover from the classical (Fox) limit to the free volume (Kovacs) regime occurred at about 0.76, in close agreement with the value of 0.72 predicted by the Kovacs equation. It should be noted that this is one of the first successful applications of the Kovacs theory to predict the T_g–composition dependence for a semicrystalline/semicrystalline blend system.

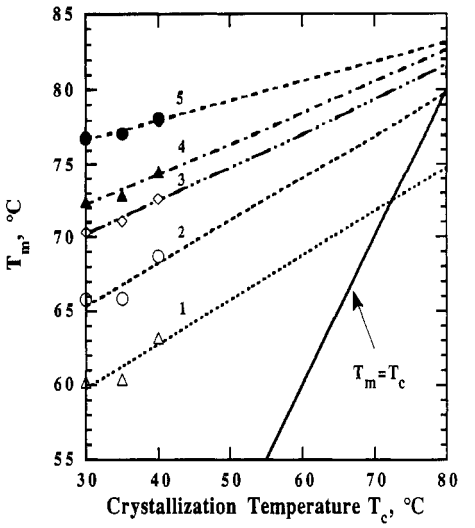

Figure 6. Determination of equilibrium melting $T_m°$ from the Hoffman–Weeks extrapolation. The data are successively displaced by 5 °C to be able to discern the different compositions. (1) 100% PCL; (2) 90% PCL; (3) 80% PCL; (4) 70% PCL; (5) 60% PCL.

Melting Point Depression. As discussed earlier, melting point depression is used extensively to evaluate the miscibility of polymer blends. These are two basic origins of melting point depression: (1) morphological and (2) thermodynamic. Morphological variables such as lamellar thickness and crystal perfection can profoundly affect the melting point. Two different approaches are often employed to obtain the equilibrium melting point $T_m°$. The first is the Gibbs–Thompson approach in which the $T_m°$ is obtained from the intercept of a plot of the reciprocal of lamellar thickness versus T_m. The more popular approach is the Hoffman–Weeks extrapolation in which $T_m°$ is derived from a plot of T_m versus T_c. Specifically, the equilibrium melting point is obtained from the intercept of the experimental T_m versus T_c curve with the $T_m = T_c$ equation. A series of Hoffman–Weeks plots is depicted in Figure 6, and the corresponding $T_m°$, derived from extrapolation, as a function of composition is illustrated in Figure 7.

According to the Nishi and Wang formulation,[12] the interaction energy density B, defined below

$$B = \frac{\chi V_{1u}}{RT} \tag{8}$$

where χ is the polymer–polymer interaction parameter and V_{1u} is the molar volume of the amorphous polymer, is related to the melting point depression by the following expression:

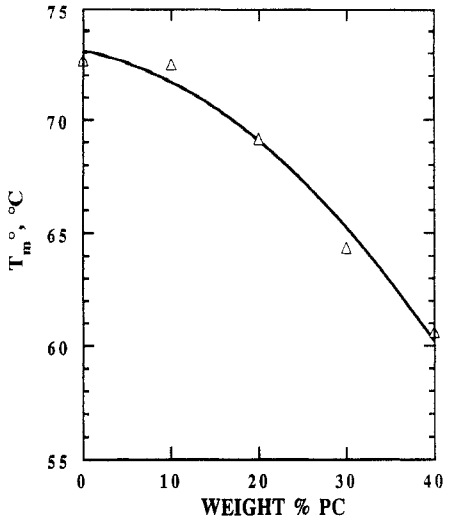

Figure 7. Equilibrium melting point $T_m°$ versus volume fraction of PC.

$$\frac{1}{V_1}\left[\frac{1}{T_m}-\frac{1}{T_m°}\right]=-\frac{BV_{2u}}{\Delta H_{2u}}\left(\frac{V_1}{T_m}\right) \tag{9}$$

where $T_m°$ is the equilibrium melting point of the pure polymer, T_m is the equilibrium melting point of the blend, ΔH_{2u} is the enthalpy of fusion per mole of repeating unit, and V_1 is the volume fraction of the amorphous polymer. Assuming B or χ is composition independent, a plot of $(1/V_1)[(1/T_m) - (1/T_m°)]$ versus (V_1/T_m) should yield a straight line with a slope which is proportional to B and a zero y-intercept. Figure 8 shows such a melting point depression plot. An examination of this figure indicates that the curve deviates from linearity and has a nonzero y-intercept. This nonlinear behavior could imply that χ is composition dependent. As discussed and demonstrated by many groups,[4,27] the errors associated with the melting point depression analysis could be significant and a small uncertainty in the melting point could profoundly affect the χ value. Hence, no attempts were made to extract χ from the melting point depression analysis as the melting point measurements and the Hoffman–Weeks extrapolations are plagued with many problems. However, Figure 7 indeed shows a melting point depression, and this could suggest a negative value for χ.

Thermal Stability. In order to investigate the thermal stability of the blends, TGA was used to measure the onset degradation temperature of the blends in air. FTIR and ^{13}C NMR were employed to probe the chemical integrity of the blends after exposure to elevated temperatures. Elucidation of the exact nature of the degradation products and mechanisms of the PCL/PC blends is highly complex and is beyond the scope of this study. Hence, the focus of the following discussion is to illustrate some basic qualitative features pertaining to the thermal stability of the blends.

The TGA scans recorded in air are depicted in Figure 9, and the corresponding onset degradation temperature as a function of composition is summarized in Figure 10. A cursory examination of these figures reveals that the onset temperature increased with increasing PC. It is observed that the onset temperature increased almost linearly with increasing PC for the PCL-rich blends and increased very modestly for the PC-rich blends. According to Figure 9, the PCL-rich blends exhibited weight loss profiles similar to that of the pure PCL. Interestingly, a two-step weight loss mechanism was observed in the PC-rich blends. Addition of even 10% PCL to PC strongly

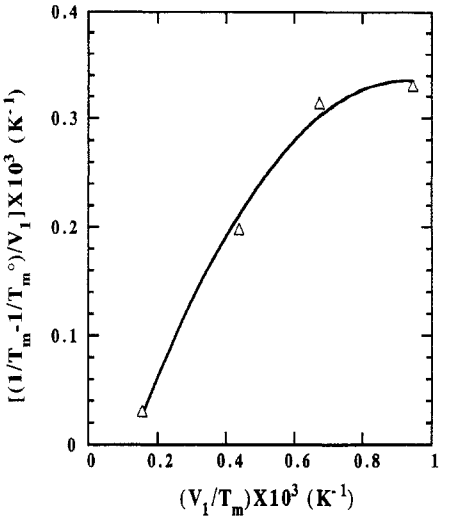

Figure 8. Melting point depression plot, where T_m is the melting point of PCL crystals in the blends, $T_m°$ is the melting point of pure PCL, and V_1 is the volume fraction of PC.

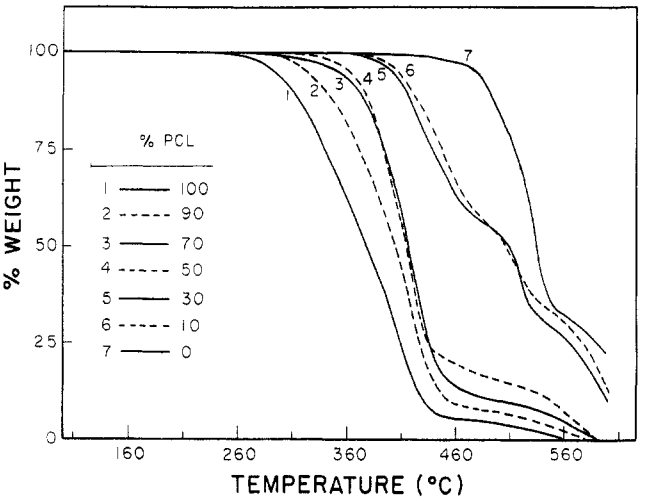

Figure 9. TGA curves for PCL/PC blends heated at 10 °C/min in air.

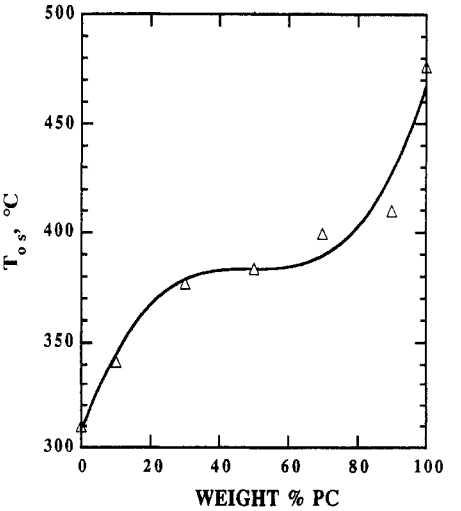

Figure 10. Onset degradation temperature for PCL/PC blends in air.

modified the degradation profile and significantly lowered the degradation temperature.

It was observed that the blends liberated a large amount of bubbles when they were heated to temperatures close to the LCST (~260 °C). The chemical nature of these bubbles was identified by FTIR. Figure 11 shows the FTIR

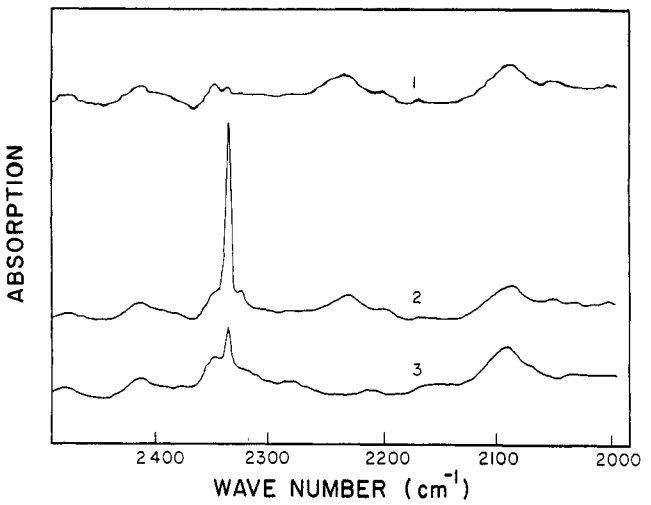

Figure 11. FTIR spectra for (3) pure PCL and (2) a 75% PCL/25% PC blend, both exposed to 280 °C for 5 min, and (1) a 75% PCL/25% PC blend without exposure to elevated temperatures. Carbon dioxide absorption occurs at 2340 cm^{-1}.

spectra for pure PCL and 25% PC/75% PCL blends. Strong carbon dioxide (CO_2) absorption at 2340 cm^{-1} was observed for samples heated at 280 °C for 5 min. At elevated temperatures close to the LCST, it is known that PCL could undergo chain scission, resulting in the formation of CO_2. Furthermore, polyester blends[28] can undergo transesterification which could also produce CO_2 as a byproduct. In order to suppress thermally-induced chain scission, a 50% PCL/50% PC blend was prepared at 250 °C for 10 min in the presence of a 2 wt % titanium butoxide trans-reaction catalyst under nitrogen for NMR study. Results derived from the ^{13}C NMR study indicated no signs of transesterification as the spectrum for the samples exposed to elevated temperature, and the trans-reaction catalyst remained virtually intact. The FTIR results coupled with the NMR findings suggested that the blend degradation, as detected by the evolution of CO_2, primarily came from chain scission of PCL. This hypothesis is consistent with the thermooxidative chain-branching mechanism previously proposed.[4]

Small-Angle Neutron Scattering. Since the LCST for the PCL/PC system overlaps with the degradation temperatures, determination of the cloud-point curve using the conventional optical measurement is complicated by the evolution of CO_2. Generally, the spinodal curve could be obtained by examining the temperature dependence of the correlation length derived from the SANS profiles.[29] Additionally, the interaction parameter χ may be calculated from the SANS profiles using the random-phase approximation (RPA)[30] analysis as illustrated below:

$$\frac{K_n}{I(q)} = \frac{1}{N_A V_A \phi_A D_A(qR_{gA})} + \frac{1}{N_B V_B \phi_B D_B(qR_{gB})} - \frac{2\chi}{V_0} \quad (10)$$

where $I(q)$ is the absolute scattering intensity, $q = 4\pi\lambda^{-1}\sin(\theta/2)$, θ being the scattering angle, N_i the degree of polymerization of component i, V_i the monomer volume, ϕ_i the volume fraction, V_0 the "cell" or the reference volume, K_n and $D_i(qR_{gi})$ are the contrast factor and the Debye scattering function, respectively, which are defined as

$$K_n = \left(\frac{a_A}{V_A} - \frac{a_B}{V_B}\right)^2 N_{av} \quad (11)$$

$$D_i(qR_{gi}) = \frac{2}{U_i^2}[\exp(-U_i) - 1 + U_i] \quad (12)$$

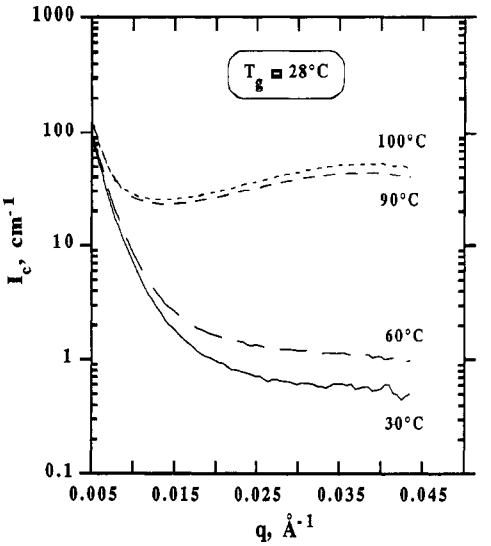

Figure 12. SANS profiles for a 70% d-PC/30% PCL blend.

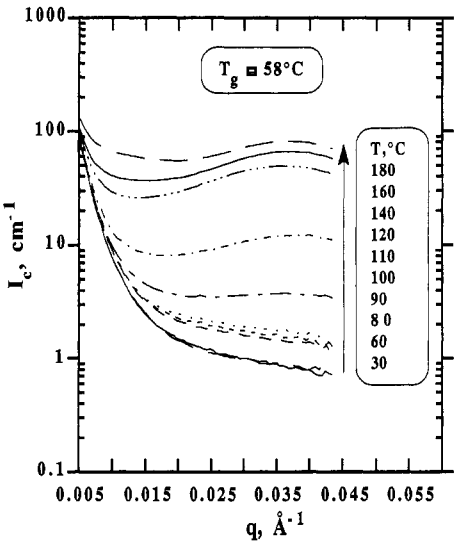

Figure 13. SANS profiles for a 80% d-PC/20% PCL blend.

where a_i/V_i is the scattering length density, N_{av} is Avogadro's number, $U_i = q^2R_{gA}^2$, and $R_{gi} = N_A b_A^2/6$, b_i being the segment length of component i. In order to reduce the number of floating parameters, an average segment length b_{ave} is often used and defined as

$$b_{ave} = b_i(V_0/V_i)^{1/2} \quad (13)$$

Effectively, the RPA analysis reduces to fitting the SANS profiles with two adjustable parameters χ/V_0 and b_{ave}.

As discussed earlier, the PC in the PCL-rich blends is semicrystalline and becomes totally amorphous at about 230 °C. Since the PCL/PC blends were not thermally stable at these elevated temperatures, SANS studies of amorphous/amorphous blends were limited to the PC-rich blends where PC crystallization is highly suppressed. The SANS profiles as a function of temperature for three d-PC rich blends are shown in Figures 12–14. It is readily observed that the scattering intensity first remained fairly constant with increasing temperature and then increased significantly at temperatures above the blend T_g. This sudden rise in the scattering intensity was mainly caused by crystallization of PC, resulting from prolonged annealing, since the temperature was ramped in a stepwise fashion. This finding implies that χ cannot be easily extracted from the SANS profiles measured above the blend T_g due to PC crystallization.

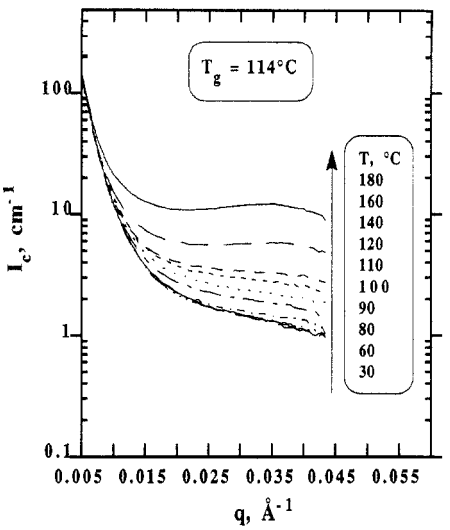

Figure 14. SANS profiles for a 90% d-PC/30% PCL blend.

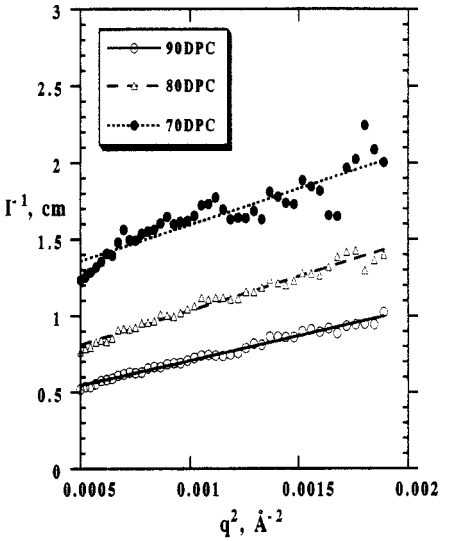

Figure 15. Random-phase approximation (RPA) fit to the SANS profiles measured at 30 °C.

Attempts were made to estimate χ from SANS recorded below the blend T_g. The analysis assumes that the scattering predominantly arises from concentration fluctuations. Figure 15 shows the RPA fit to the SANS profiles recorded at 30 °C. The corresponding χ/V_0 and b_{ave} are plotted in Figure 16. These RPA results suggested a composition-dependent χ and that the blend interactions are favorable as reflected by the negative sign of the interaction parameter. Assuming the cell volume to be approximated by $V_0 = (V_A V_B)^{1/2}$, χ is estimated to be on the order of −1 which is in agreement with previous results[3] derived from the melting point depression analysis. However, it is extremely important to stress that the χ measured below T_g represents a nonequilibrium value which may not reflect the true value. Additionally, the interpretation of the RPA results is further complicated by the possible residual crystallinity in the samples.

Conclusions

The PCL/PC blends exhibited multiple phase transitions and highly complex phase behavior. It was found that the PCL-rich blends are semicrystalline/semicrystalline at room temperature in which both components readily undergo crystallization. At about 30% PC incorporation, the PCL crystallinity showed a marked reduction, whereas the PC crystallinity approached a maximum. On the basis of the degree of crystallinity of both components

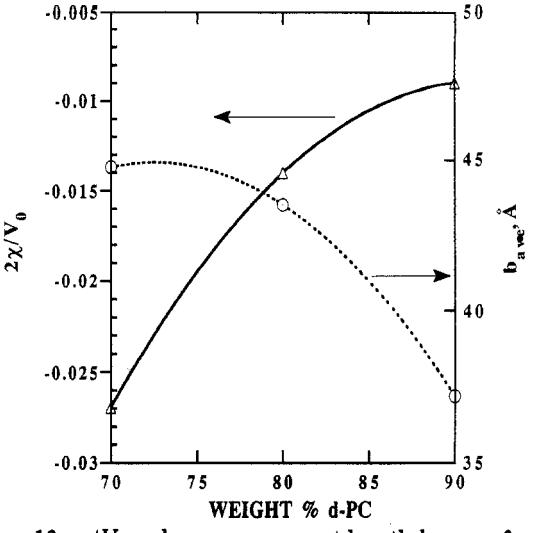

Figure 16. χ/V_0 and average segment length b_{ave} as a function of composition at 30 °C, where V_0 is the "cell" volume.

measured from DSC, the real composition of the amorphous phase was calculated. The composition dependence of T_g exhibited a discontinuity (cusp) and was critically examined using the classical equations of Gordon–Taylor and Fox and the free volume formulation of Braun–Kovacs. The Gordon–Taylor equation failed to reproduce the cusp observed in the T_g–composition dependence. However, combination of the Fox and Braun–Kovacs equations accurately reproduced the cusp and yielded a very good fit to the T_g–composition data. The experimental crossover volume fraction (of PC) from the classical (Fox) limit to the free volume (Kovacs) regime was about 0.76, in very close agreement with the critical value of 0.72 predicted by Kovacs theory. This is one of the first successful applications of Kovacs theory to a semicrystalline/semicrystalline blend system.

Thermal stability of the blends was evaluated with TGA. The onset degradation temperature increased with increasing PC. At temperatures close to the LCST (~260 °C), carbon dioxide evolution was observed and detected by FTIR. ^{13}C NMR studies indicated that the blends were not susceptible to transesterification as the spectrum remained virtually unchanged for samples exposed to elevated temperature and a titanium butoxide catalyst which is known to promote trans-reaction in polyester blends. These findings suggested that the blends degraded primarily via chain scission of PCL as evidenced by the evolution of carbon dioxide.

In contrast to other studies,[4] the PCL-rich blends showed melting point depression as revealed by the Hoffman–Weeks extrapolations. SANS studies on the d-PC-rich blends indicated that the scattering intensity first remained fairly constant with increasing temperature and then increased sharply at temperatures above the blend T_g. This rise in the intensity was attributed to the crystallization of PC, resulting from prolonged annealing. Attempts were made to estimate χ from the SANS profiles measured at 30 °C (below T_g) using the RPA analysis. The SANS results coupled with the melting point depression analysis suggested favorable blend interactions as reflected by the negative sign of the interaction parameter.

Acknowledgment. Support of this work by Novacor Inc. is gratefully acknowledged. The authors thank B. Hammouda of NIST for help with the SANS measurements, H. E. Yang and P. Yazobucci of Eastman Kodak Co. for the deuterated polycarbonate synthesis, and F. Ignatious of UMass for the NMR measurements.

References and Notes

(1) Koleske, J. V. In *Polymer Blends*; Paul, D. R., Newman, S., Eds.; Academic Press: New York, 1978.
(2) Cruz, C. A.; Paul, D. R., Barlow, J. W. *J. Appl. Polym. Sci.* **1979**, *23*, 589.
(3) Varnell, D. F.; Runt, J. P.; Coleman, M. M. *Macromolecules* **1981**, *14*, 1350.
(4) Jonza, J. M.; Porter, R. S. *Macromolecules* **1986**, *19*, 1946.
(5) Cheung, Y. W.; Stein, R. S.; Chu, B.; Wu, G. Submitted to *Macromolecules*, submitted.
(6) Cheung, Y. W.; Stein, R. S., in preparation.
(7) Cheung, Y. W.; Stein, R. S.; Wignall, G. D.; Yang, H. E. *Macromolecules* **1993**, *26*, 5365.
(8) Cheung, Y. W.; Stein, R. S.; Wignall, G. D.; Lin, J. S. *Macromolecules*, following paper in this issue.
(9) Cruz, C. A.; Barlow, J. A.; Paul, D. R. *Macromolecules* **1979**, *12*, 726.
(10) Coleman, M. M.; Painter, P. C. *J. Appl. Spectrosc. Rev.* **1984**, *20* (3 & 4), 255.
(11) Coleman, M. M.; Zarian, J. *J. Polym. Sci., Polym. Phys. Ed.* **1979**, *17*, 837.
(12) Nishi, T.; Wang, T. T. *Macromolecules* **1975**, *8*, 909.
(13) Olabisi, O. *Macromolecules* **1975**, *8* (3), 316.
(14) Shibayama, M.; Yang, H. E.; Stein, R. S.; Han, C. C. *Macromolecules* **1985**, *18*, 2179.
(15) Han, C. C.; Baurer, B. J.; Clark, J. C.; Muroga, Y.; Okada, M.; Tran-Cong, Q.; Sanchez, I. C. *Polymer* **1988**, *29*, 2002.
(16) Brandrup, J.; Immergut, E. H. *Polymer Handbook*, 2nd ed.; Wiley: New York, 1975.
(17) Khamatta, F. B.; Warner, F.; Russell, T. B.; Stein, R. S. *J. Polym. Sci. Polym. Phys. Ed.* **1976**, *14*, 1391.
(18) Wignall, G. D., Fates, F. S. *J. Appl. Crystallogr.* **1987**, *20*, 28.
(19) Solc, K., Ed. *Polymer Compatibility and Incompatibility: Principles and Practices*; Harwood Academic: New York, 1982.
(20) Fox, T. G.; Flory, P. J. *J. Polym. Sci.* **1954**, *14*, 315.
(21) Couchman, P. R.; Karasz, F. E. *Macromolecules* **1978**, *11*, 117.
(22) Utracki, L. A. *Adv. Polym. Technol.* **1985**, *5*, 33.
(23) Gordon, M.; Taylor, J. S. *J. Appl. Chem.* **1952**, *2*, 493.
(24) Aubin, M.; Prud'homme, R. E. *Macromolecules* **1988**, *21*, 2945.
(25) Kovacs, A. J. *Adv. Polym. Sci.* **1963**, *3*, 394.
(26) Braun, G.; Kovacs, A. J. In *Physics of Non-Crystalline Solids*; Prins, J. A., Ed.; North-Holland: Amsterdam, The Netherlands, 1965.
(27) Koningsveld, R. Private communications.
(28) Godard, P.; Dekoninck, J. M.; Devlesavedr, J. *J. Polym. Sci., Polym. Chem.* **1986**, *24*, 3315.
(29) Beaucage, G. Ph.D. Thesis, University of Massachusetts at Amherst, Amherst, MA, 1991.
(30) de Gennes, P.-G. *Scaling Concepts in Polymer Physics*; Cornell University: Ithaca, NY, 1979.